

Supporting Information for

Molecular crystalline capsules that release their contents by light

Akira Nagai, Ryo Nishimura, Yohei Hattori, Eri Hatano, Ayako Fujimoto, Masakazu Morimoto,
Nobuhiro Yasuda, Kenji Kamada, Hikaru Sotome, Hiroshi Miyasaka, Satoshi Yokojima, Shinichiro
Nakamura, Kingo Uchida

Correspondence to: uchida@rins.ryukoku.ac.jp

Table of Contents

1. Materials and Methods.....	S1-S3
2. Synthesis and photochromic reaction of diarylethene	S4
3. Crystalline capsules recrystallized from other solvents and crystalline capsule including BPEA crystal.....	S5
4. Release of fluorescent matters from crystalline capsules.....	S6
5. Temperature increase by femtosecond laser.....	S7
6. Crystal packing of 1o molecules and conceptual diagram of the expansion and contraction of each axis of the crystal.....	S8
7. Photoresponsive behavior of 1o crystal upon polarized UV irradiation.....	S9
8. Crystallographic information.....	S10-S12
9. Explanations of supplementary movies	S13-S14

Materials and Methods

Instruments

Melting points were measured on the Yanaco MP-500D. The JEOL RESONANCE JNM-ECS400 spectrometer was used for the NMR measurements. Chemical shifts are given in parts per million (p.p.m.) using the TMS and solvent signals (TMS (^1H NMR: 0.00 ppm), CHCl_3 (^{13}C NMR: 77.16 ppm), and C_6F_6 (^{19}F NMR: -164.9 ppm)) as references. Absorption spectra of the solutions were monitored on the Hitachi U-4150 spectrophotometer. The Perkin Elmer DSC8500 was used for DSC measurement, with a rate of elevating temperature of $10\text{ }^\circ\text{C} / \text{min}$. For observation of the capsuled and non-capsuled crystals, we used the polarized optical microscope OPTIPHOT2-POL (Nikon Japan), the Moticam 2000 2.0M Pixel USB2.0 camera (Shimadzu), and the KEYENCE digital microscopes VH-S30, VH-S1, and VH-Z450. For cross-section observation of crystalline capsules, we used a scanning electron microscope (KEYENCE VE-8800). For the UV light irradiation, the SPECTROLINE (SPECTRO NICS, MODEL EB-280C/J, $\lambda=312\text{ nm}$) and KEYENCE UV-LED UV-400 with a UV-50H attachment ($\lambda = 365\text{ nm}$, $500\text{ mW}/\text{cm}^2$ or $400\text{ mW}/\text{cm}^2$) were used. For visible light irradiation, we used the 500W USHIO SX-UI501XQ xenon lamp equipped with Toshiba color filters (Y-50, Y-48, Y-44, UV-29 or Y-44, UV-29). Quantum yields of the cyclization and cycloreversion reactions of **1o** and **1c** were measured using a homemade setup. Light irradiation was carried out in 1-cm path quartz cuvettes under continuous stirring, using a mercury lamp (500 W USHIO optical module H500) at 313 nm and a xenon lamp (500W USHIO SX-UI501XQ) at 578 nm as irradiation sources.

Isolation of the closed-ring isomer 1c

For the X-ray crystal analysis of **1c**, closed-ring isomer **1c** was isolated. Crystalline powder of **1o** (140 mg) was dissolved in 7000 mL of hexane. Each 70 mL portion of the solution was stored in a 100-mL glass tube and irradiated with 312 nm of UV light for 150 s to make a photostationary state (PSS) with a ratio of **1o**:**1c**=1:99. The procedure was repeated 99 times. The PSS solutions were combined, and the solvent was removed in vacuo. The obtained mixture was purified by recrystallization from hexane to obtain a pure crystal of **1c**.

^1H NMR (400 MHz, CDCl_3) δ 0.31 (s, 18H), 2.19 (s, 6H), 7.26 (s, 2H), 7.34 (t, $J = 7.5\text{ Hz}$, 2H), 7.57 (d, $J = 7.5\text{ Hz}$, 2H), 7.58 (d, 2H, $J = 7.5\text{ Hz}$), 7.65 (s, 2H); ^{19}F NMR (376 MHz, CDCl_3 , ppm) δ -136.7 (s, 2F), -116.0 (q, 4F).

Single-crystal X-ray diffraction (XRD) analysis

X-ray crystallographic analyses for bulk crystals of **1o**, **1o-UV** irradiated with $\lambda = 400\text{ nm}$ light for 20 sec (EXFO Omni Cure LX400), and **1c** were performed with an X-ray diffractometer (Bruker AXS, D8 QUEST) with $\text{Mo K}\alpha$ radiation ($\lambda = 0.71073\text{ \AA}$). The crystals were cooled using a low temperature controller (Japan Thermal Engineering, JAN 2-12). The diffraction frames were integrated with the Bruker SAINT program. The cell constants were determined by global refinement. The data were corrected for absorption effects using a multi-scan method (SADABS). The structure was solved by the direct method and refined by the full-matrix least-squares method using the SHELX-2014 program. The positions of all hydrogen atoms were calculated geometrically and refined by the riding model. The crystallographic data can be obtained free of charge from The Cambridge Crystallographic Data Centre via www.ccdc.cam.ac.uk/structures. (CCDC 1983516, 1983522, 1983523, 1983529).

X-ray crystallographic analysis for the crystalline capsule of **1o** and **1o (BPEA)** was carried out at the BL02B1 and BL40XU beamlines of SPring-8. Beamline BL02B1: an Si(311) double crystal monochromator was used with wavelengths of 0.4146 Å, and 0.4298 Å; the sizes of the X-ray beams were 127 (H) × 120 (V) μm, and 127 (H) × 131 (V) μm, respectively. The diffractometer was equipped with a PILATUS3 X CdTe 1M detector (DECTRIS Ltd., Baden, Switzerland) from 20 to 173 K. Beamline BL40XU: an Si(111) channel-cut monochromator was used, and the wavelength and size of the X-ray beam were 0.8108 Å and 75 × 75 μm, respectively. The diffraction data were collected by the oscillation method using an EIGER detector at 173 K. The data were corrected for absorption effects by a multi-scan method with ABSCOR. The structure was solved by the direct method and refined by the full-matrix least-squares method using the SHELX-2014/7 program. The positions of all hydrogen atoms were calculated geometrically and refined by the riding model. The crystallographic data can be obtained free of charge from The Cambridge Crystallographic Data Centre via www.ccdc.cam.ac.uk/structures. (CCDC 1983524, 1983525, 1983556, 1983598, 2040178, 2040177).

Introduction of fluorescent beads inside the crystalline capsules

As fluorescent beads, we purchased Fluoresbrite Plain Microspheres (2.5% Solids-Latex), 1.0 μm YG (code: 17154) from Polysciences, Inc. and filled them into crystalline capsules prepared by recrystallization from a hexane solution. We cut both sides of the crystal capsules. Then the beads were dispersed in water and introduced through a capillary phenomenon by dipping an edge of the crystal. After drying the crystals by keeping them one day at ambient condition, the photosolvent experiments were carried out by irradiation with UV light (Figure S3a, $\lambda = 313$ nm, UV hand lamps SPECTROLINE Model EB-280C/J).

Multiphoton excitation experiment using a femtosecond laser system

A femtosecond laser system was used for multiphoton excitation of the sample. The light source was a Ti: Sapphire regenerative amplifier (Spectra-Physics, Spitfire, 802 nm, 100 fs, 1 W, 1 kHz) seeded by a Ti: Sapphire oscillator (Spectra-Physics, Tsunami, 802 nm, 100 fs, 820 mW, 80 MHz). A portion of the output was irradiated to the sample at an incident angle of ca. 50 degrees and focused with a plano-convex lens with a focal length of 150 mm (OptoSigma, SLSQ-30-150P). The laser spot was elliptical at the surface of the sample, and its long and short axial lengths were evaluated as 2.15 mm and 1.64 mm, respectively, from scattering images. The polarization of the laser pulses was rotated by a Berek variable waveplate (Newfocus, Model 5540) so that it would be parallel to the short axis of the molecule in the single crystal. The irradiation power was adjusted with a variable neutral-density filter (OptoSigma, NDHN-100), and typically at 300 μJ/pulse.

Measurement of two-photon absorption (TPA) cross section of **1o** in solution

The TPA cross section of **1o** was measured in dichloromethane solution by the open-aperture Z-scan method at 802 nm. An optical parametric amplifier (Spectra-Physics TOPAS Prime) pumped by a femtosecond Ti:Sapphire regenerative amplifier was used as a light source. The incident power was changed for the range of 0.55 to 1.2 mW with a repetition rate of 1 kHz and a pulse width of 100 fs. The Rayleigh range of the setup was 7.4 mm, which was sufficiently longer than the pathlength of the optical cell used (2 mm). The on-axis optical intensity at the focal point was varied for 180–370 GW/cm². Even with a high concentration (30 mM), the obtained TPA signal was close to the background. The best estimation of the cross section was $\sigma^{(2)} = 0.4 \pm 0.3$ GM (here, 1 GM = 10⁻⁵⁰ cm⁴ s molecule⁻¹ photon⁻¹) with the solution.

Estimation of excitation ratio of **1o** by femtosecond NIR laser

Based on the obtained value of $\sigma^{(2)}$, the ratio of the number of **1o** molecules excited by TPA for the photosolient experiment with a femtosecond laser was calculated as follows. The numbers used for the calculation are summarized in Figure S4d.

From the $\sigma^{(2)}$ value, the TPA coefficient β of the **1o** crystal was calculated as

$$\beta = \frac{\sigma^{(2)}N}{E_{ph}} = 1.91 \times 10^{-11} \text{ cm W}^{-1}$$

and two-photon absorbance q at the experimental condition was obtained as

$$q = \beta IL = 5.15 \times 10^{-3}$$

Then, the absorptance A by TPA is estimated as

$$A = 1 - \frac{1}{1 + q} = 5.13 \times 10^{-3}$$

Photon flow density (flux) F used for the experiment by TPA was

$$F = \frac{I}{E_{ph}} = 1.09 \times 10^{29} \text{ photons s}^{-1} \text{ cm}^{-2}$$

Using these values, the number density of molecules excited by a single femtosecond laser pulse (N_{ex}) was obtained as,

$$N_{ex} = \frac{A F t_p}{2L} = 2.79 \times 10^{15} \text{ molecules cm}^{-3}$$

With the number density of the crystal N , herein, the ratio of excited molecules by TPA was calculated as,

$$\frac{N_{ex}}{N} = 2.36 \times 10^{-6}$$

Or more simply, the transition rate by TPA was

$$w = \frac{1}{2} \sigma^{(2)} F^2 = 2.37 \times 10^7 \text{ s}^{-1}$$

Thus, within the pulse width, the ratio of excited molecules is

$$\frac{N_{ex}}{N} = w t_p = 2.37 \times 10^{-6}$$

Measurement of polar plot of action spectrum

The polarizer was placed so that the polarization direction would be parallel to the long axis of the crystal of **1o** ($\theta = 0^\circ$). Transmittance of 601 nm light before and after UV irradiation for 1.0 s (T_0 and T_1 , respectively, $\lambda = 365 \text{ nm}$, 165 mW / cm^2) was measured, and the produced **1c** was converted back to **1o** by irradiation with Xe lamp that cuts $\lambda < 480 \text{ nm}$ -light for 10 min. The polarizer was rotated by 15° , and the same measurements were repeated. The absorbance ($\log T_0/T_1$) was calculated for each angle and plotted in polar coordinates (Figure 4d).

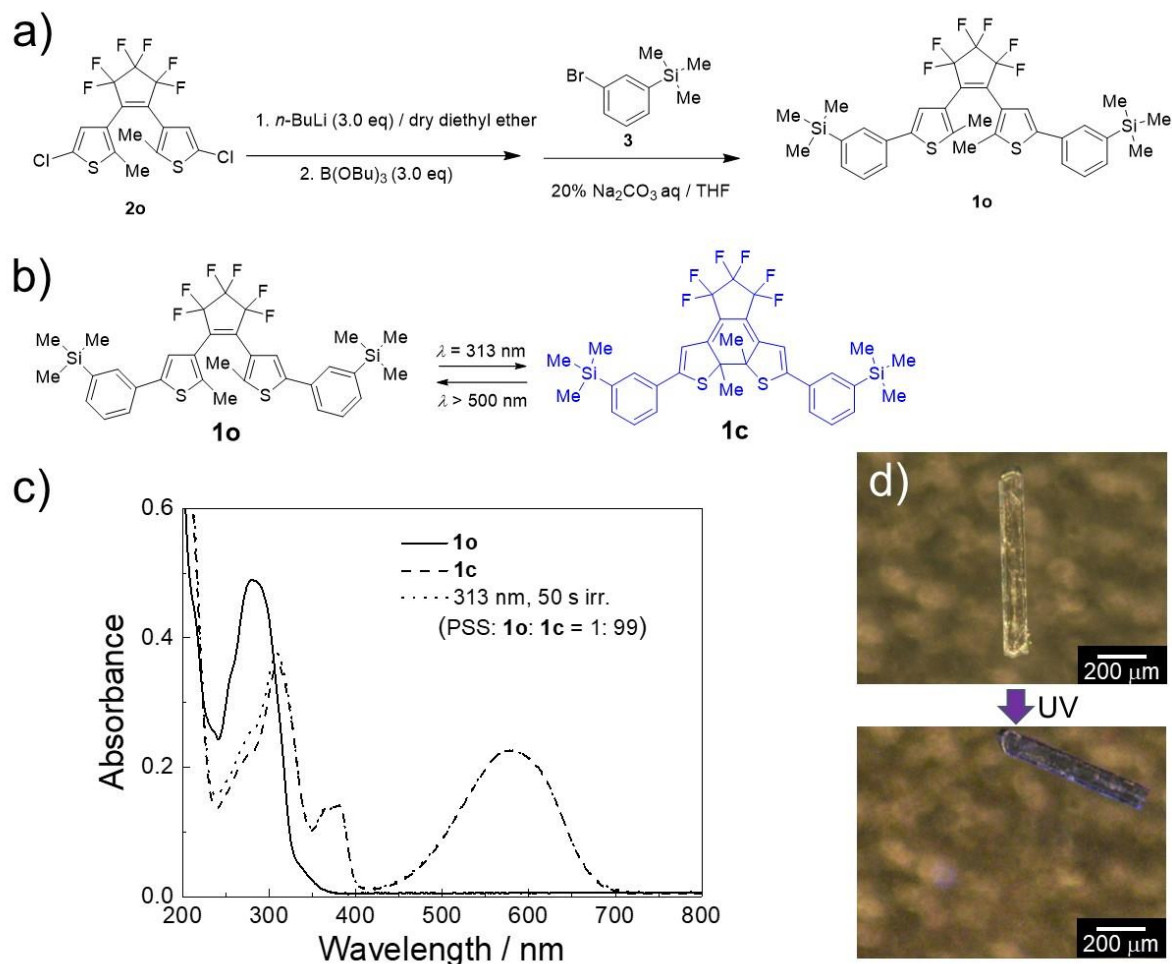


Fig. S1

Synthesis and photochromic reaction of diarylethene **1**. (a) Synthetic scheme of **1o**. (b) Molecular structures of **1o** and **1c**. (c) Absorption spectra of **1o** (solid line), **1c** (broken line), and photostationary state (PSS, **1o**: **1c** = 1: 99, dotted line) in hexane. Absorption maximum wavelength of **1o** was 284 nm ($\epsilon = 3.78 \times 10^4 \text{ M}^{-1} \text{ cm}^{-1}$). When UV light was irradiated, the solution was colored blue, and the absorption maximum of **1c** appeared at 580 nm ($\epsilon = 1.76 \times 10^4 \text{ M}^{-1} \text{ cm}^{-1}$). Then visible light was irradiated, the solution became colorless, and the absorption spectrum returned to that of **1o**. Quantum yields of cyclization and cycloreversion reactions were obtained as 0.65 and 7.9×10^{-3} , respectively. (d) Photosolient phenomena (jumping and breaking) accompanying photochromic reaction of a crystal **1o**.

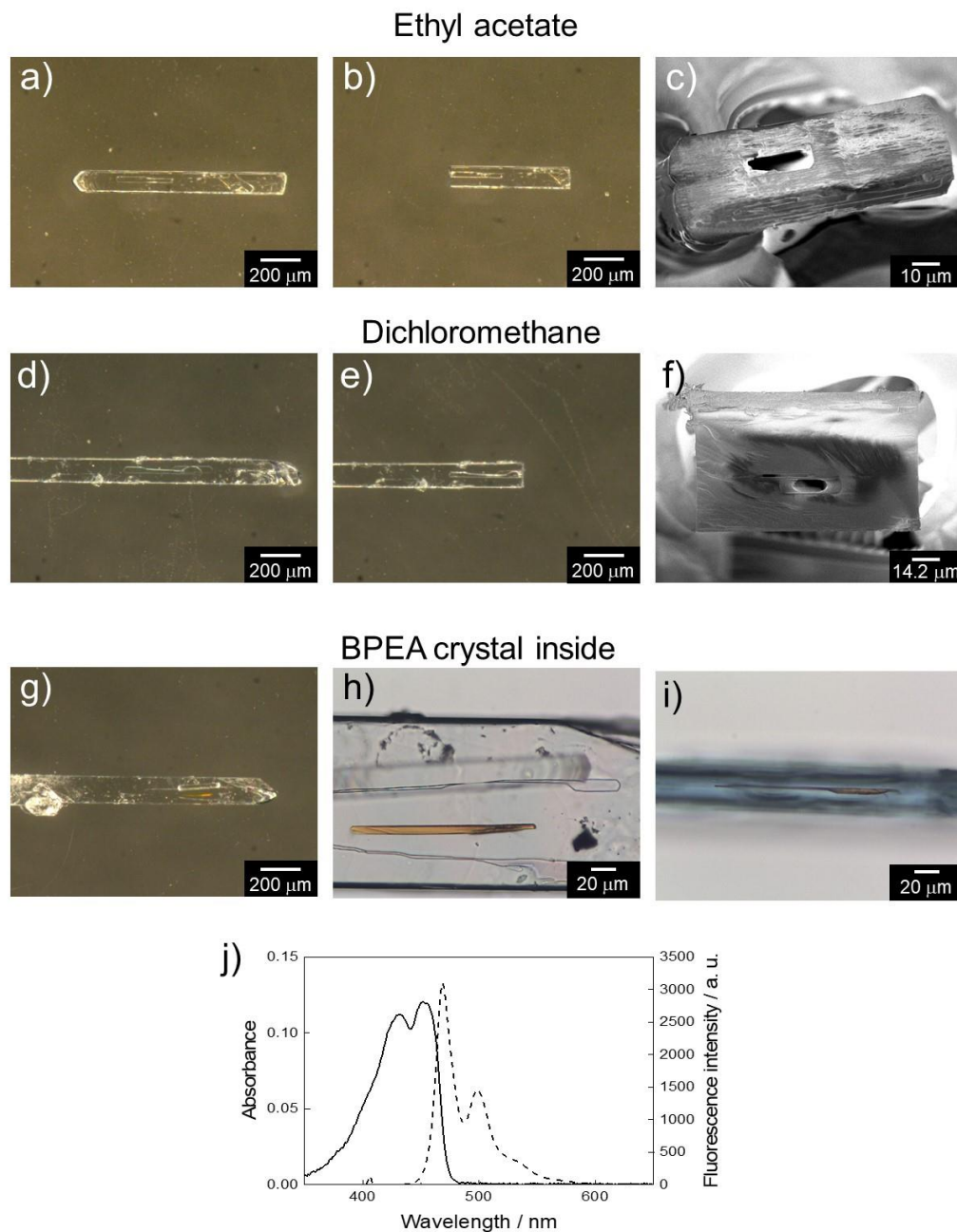


Fig. S2

Crystalline capsules recrystallized from other solvents and crystalline capsule including BPEA crystal. (a) A crystalline capsule of **1o** obtained by recrystallization from ethyl acetate solution. (b) Crystal of (a) cut at the hollow. (c) Cross-sectional SEM image of (b). (d) A crystalline capsule of **1o** obtained by recrystallization from dichloromethane solution. (e) Crystal of (d) cut at the hollow. (f) Cross-sectional SEM image. (g) Optical image of a crystal of **1o** including orange **BPEA** crystal. (h) Magnified image of the encapsulated **BPEA** crystal in **1o** crystal. (i) Side view of (h). (j) Absorption (solid line) and emission (broken line) spectra of **BPEA** in hexane.

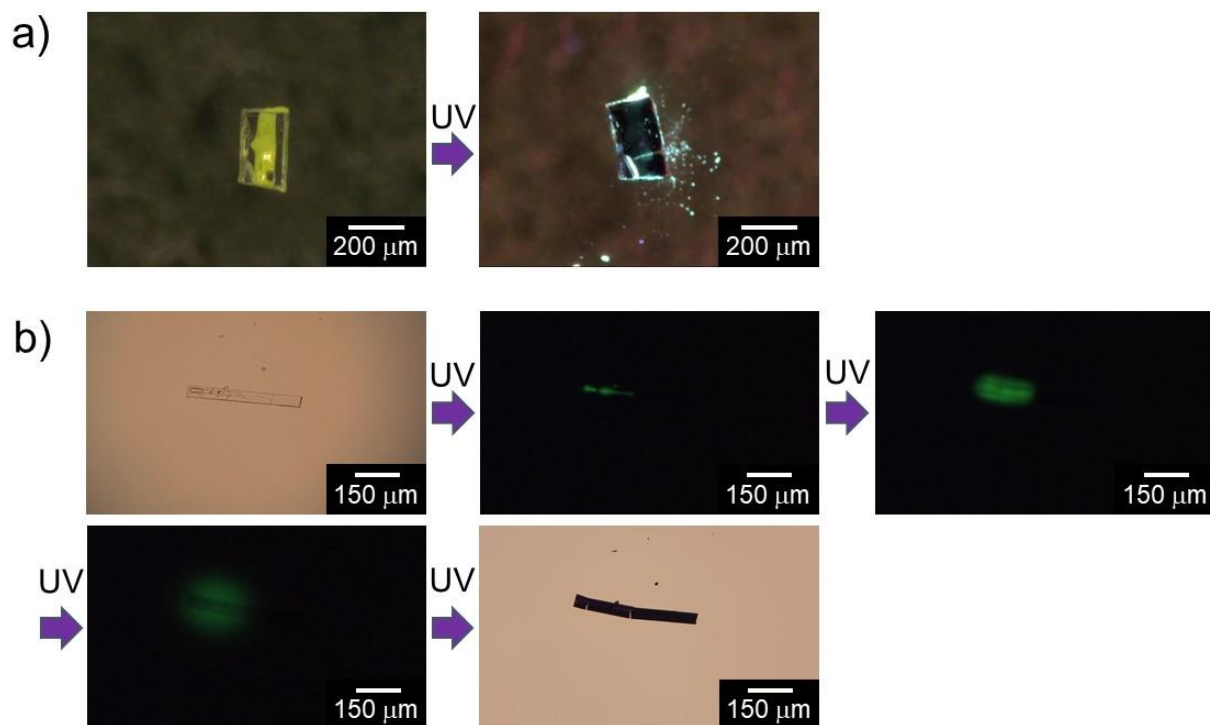


Fig. S3

Release of fluorescent matters from crystalline capsules. (a) A crystal packed with fluorescent beads of 1- μm diameter by capillary effect after breaking both ends of the crystalline capsule of **1o**. Upon UV ($\lambda = 365 \text{ nm}$, $550 \text{ mW} / \text{cm}^2$) irradiation, photoinduced breaking occurred with scattering of the packed fluorescent beads. (b) Photosolient phenomena of small crystalline capsule **1o** releasing the included solution of **5(6)-FAM** in a buffer solution ($\text{pH} = 9.18$ at $25 \text{ }^\circ\text{C}$). Upon UV irradiation, the green fluorescence expanded around the crystals. Final picture is the colored crystal after UV irradiation.

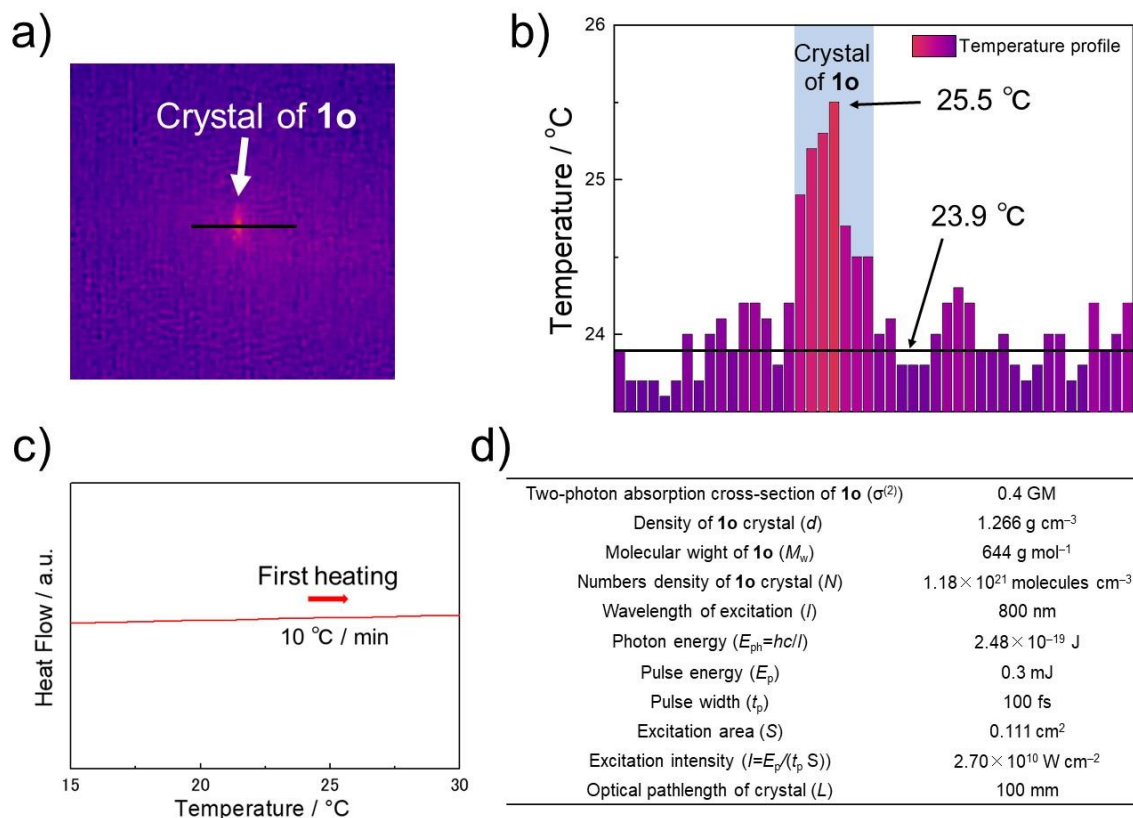


Fig. S4

Temperature increase by femtosecond laser. (a) Thermography of a crystal of **1o** during the femtosecond NIR laser irradiation. (b) Temperature profile of the crystal of **1o**. An increase of only 1.6 °C (23.9° to 25.5 °C) was monitored at the crystal. (c) DSC curve of crystals of **1o** from 15 to 30 °C. Since there was no peak in this region, the behaviors of crystals of **1o**, shown by irradiation of the femtosecond laser, are not attributed to the phase transition resulting from the rise in temperature. (d) Parameters used for calculation of the excitation ratio by two-photon absorption.

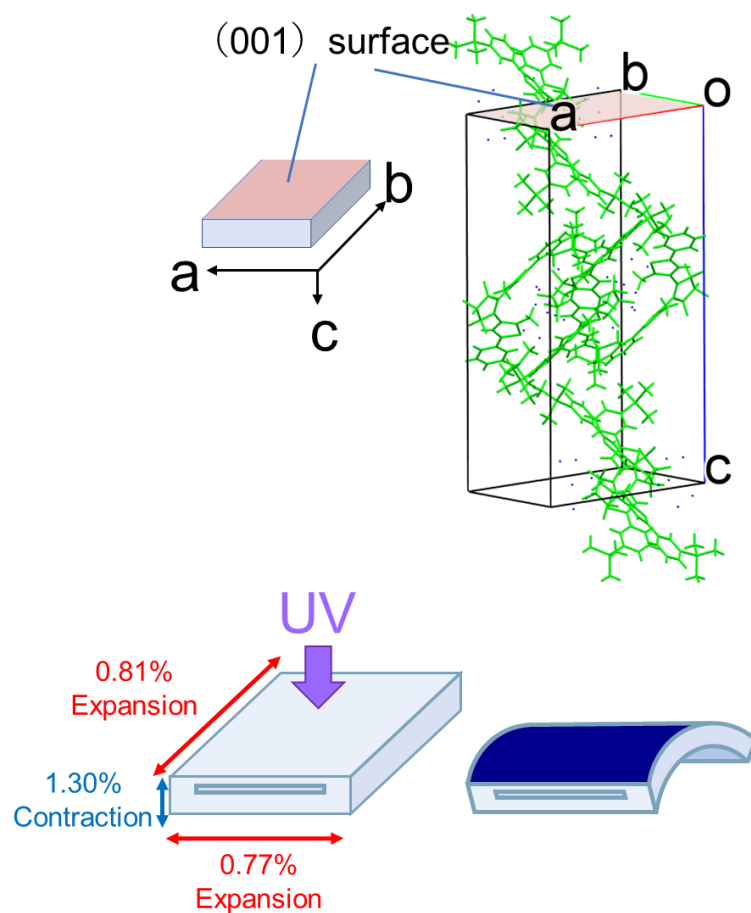


Fig. S5

Crystal packing of 1o molecules and conceptual diagram of the expansion and contraction of each axis of the crystal. The longer and shorter axes of the widest surface of the crystal were assigned to the b -axis and a -axis, respectively, and the thickness direction was assigned to the c -axis. The long axis of the crystal parallel to the b -axis further expanded. The crystals bend to the direction opposite to the light source. Finally, the crystals which could not withstand the accumulated strain were broken.

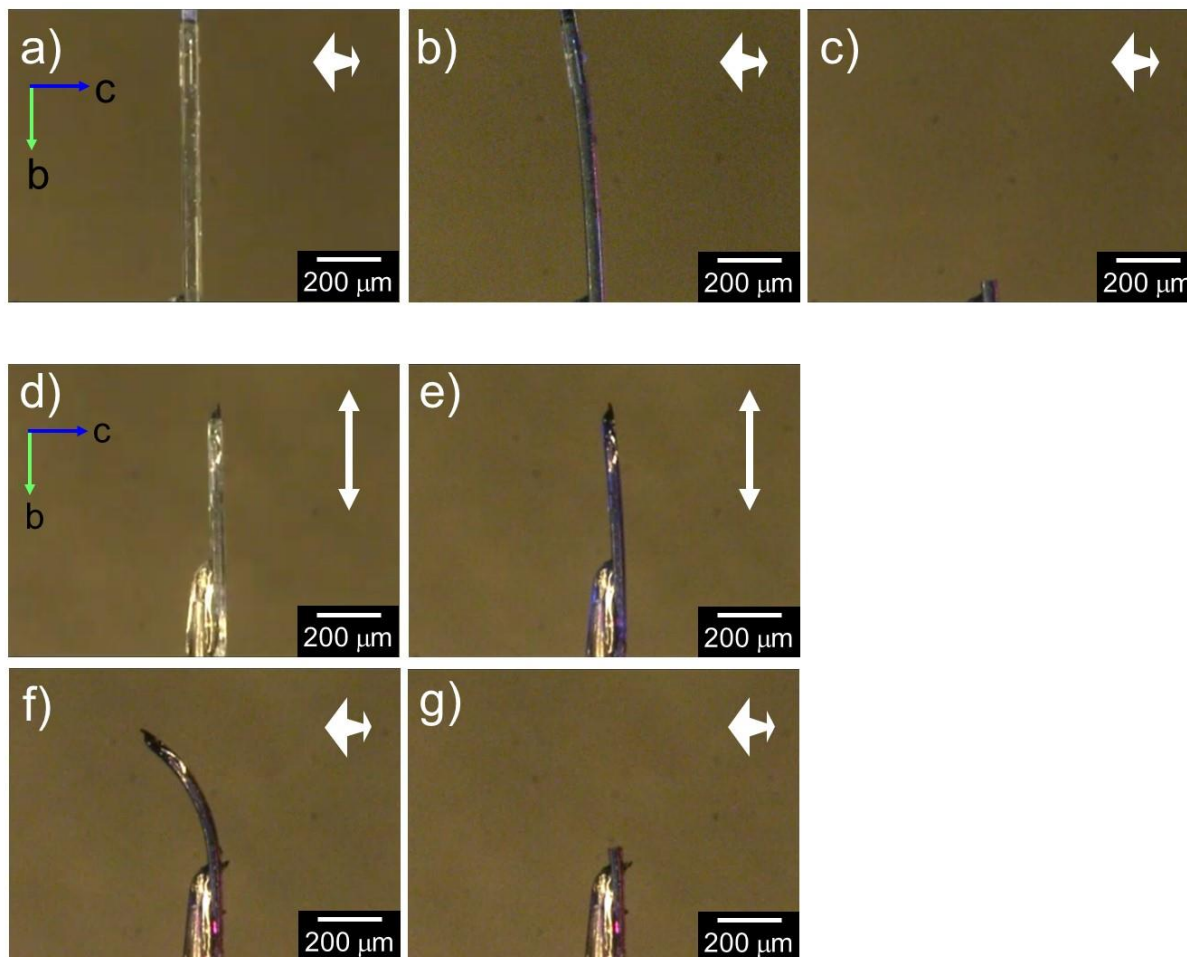


Fig. S6

Photoresponsive behavior of **1o** crystal upon polarized UV irradiation. (a) A crystalline capsule of **1o** fixed on the edge of a glass capillary viewed from the side (100) surface. (b) Upon irradiation of linearly polarized 365-nm light parallel to the *a*-axis of the crystalline capsule of **1o**, the crystal bent in the direction opposite to the light source. (c) Continued irradiation of 365-nm light broke the capsule, showing a photosalient phenomenon. (d) Another crystalline capsule of **1o** fixed on the edge of a glass capillary viewed from the side (100) surface. (e) Irradiation of linearly polarized 365-nm light parallel to the *b*-axis. Irradiation to the wide (001) surface of the crystalline capsule for 40 s slightly bent the crystal but could not break it. (f) When the linear polarizer was rotated 90° (made parallel to the *a*-axis), and the UV light was irradiated again, the crystalline capsule was bent much more. (g) Continued irradiation induced the crystal of the crystalline capsule to break, showing a photosalient phenomenon.

Table S1.

Crystal data for **1o**, **1c** with no capsule structures recrystallized from hexane, and for crystalline capsules of **1o** recrystallized from hexane, ethyl acetate, and dichloromethane.

	1o (non-capsule) recrystallized from hexane	1c recrystallized from hexane	1o capsule recrystallized from hexane	1o capsule recrystallized from ethyl acetate	1o capsule recrystallized from dichloromethane
Wavelength / Å	0.71073	0.71073	0.4298	0.8108	0.8108
Formula	C ₃₃ H ₃₄ F ₆ S ₂ Si ₂	C ₃₃ H ₃₄ F ₆ S ₂ Si ₂	C ₃₃ H ₃₄ F ₆ S ₂ Si ₂	C ₃₃ H ₃₄ F ₆ S ₂ Si ₂	C ₃₃ H ₃₄ F ₆ S ₂ Si ₂
formula weight	664.90	664.90	664.90	664.90	664.90
<i>T</i> / K	93 (2)	93 (2)	93 (2)	173 (2)	173 (2)
crystal system	Orthorhombic	Monoclinic	Orthorhombic	Orthorhombic	Orthorhombic
space group	<i>Pbcn</i>	<i>P2₁/n</i>	<i>Pbcn</i>	<i>Pbcn</i>	<i>Pbcn</i>
<i>a</i> / Å	18.1270 (13)	6.7829 (2)	18.1941 (3)	18.2337 (5)	18.2216 (5)
<i>b</i> / Å	10.9066 (6)	24.0037 (9)	10.9554 (2)	10.9971 (9)	10.9631 (8)
<i>c</i> / Å	33.637 (2)	20.7451 (8)	33.6907 (6)	33.6597 (16)	33.6434 (14)
<i>α</i> / °	90	90	90	90	90
<i>β</i> / °	90	96.5736 (13)	90	90	90
<i>γ</i> / °	90	90	90	90	90
<i>V</i> / Å ³	6650.2 (8)	3355.4 (2)	6715.4 (2)	6749.4 (7)	6720.8 (6)
<i>Z</i>	8	4	8	8	8
<i>R</i> ₁ (<i>I</i> > 2σ(<i>I</i>))	0.0465	0.0388	0.0359	0.0958	0.0709
<i>wR</i> ₂ (<i>I</i> > 2σ(<i>I</i>))	0.0929	0.0948	0.1046	0.2897	0.1957
<i>R</i> ₁ (all data)	0.0839	0.0549	0.0385	0.1208	0.0809
<i>wR</i> ₂ (all data)	0.1070	0.1049	0.1077	0.3600	0.2224
CCDC	1983516	1983529	1983524	2040178	2040177

Table S2.

Crystal data for crystalline capsule of **1o** containing **BPEA**, and capsule containing **BPEA** after 400 nm UV light irradiation for 10 second and 20 second.

	1o (BPEA)	1o (BPEA)-UV (after 313 nm light irradiation for 10 sec.)	1o (BPEA)-UV (after 313 nm light irradiation for 20 sec.)
Wavelength / Å	0.4146	0.4146	0.4146
Formula	C ₃₃ H ₃₄ F ₆ S ₂ Si ₂	C ₃₃ H ₃₄ F ₆ S ₂ Si ₂	C ₃₃ H ₃₄ F ₆ S ₂ Si ₂
formula weight	664.90	664.90	664.90
<i>T</i> / K	173 (2)	173 (2)	173 (2)
crystal system	Orthorhombic	Orthorhombic	Orthorhombic
space group	<i>Pbcn</i>	<i>Pbcn</i>	<i>Pbcn</i>
<i>a</i> / Å	18.2035 (10)	18.2294 (8) (+0.14%)	18.2491 (7) (+0.25%)
<i>b</i> / Å	10.9561 (6)	10.9740 (5) (+0.16%)	10.9875 (4) (+0.29%)
<i>c</i> / Å	33.7120 (17)	33.6809 (15) (-0.09%)	33.6440 (12) (-0.20%)
α / °	90	90	90
β / °	90	90	90
γ / °	90	90	90
<i>V</i> / Å ³	6723.5 (6)	6737.9 (5) (+0.21%)	6746.0 (4) (+0.34%)
<i>Z</i>	8	8	8
<i>R</i> ₁ (<i>I</i> > 2σ(<i>I</i>))	0.0353	0.0376	0.0535
<i>wR</i> ₂ (<i>I</i> > 2σ(<i>I</i>))	0.1048	0.1087	0.1162
<i>R</i> ₁ (all data)	0.0429	0.0481	0.0535
<i>wR</i> ₂ (all data)	0.1087	0.1134	0.1215
CCDC	1983525	1983556	1983598

Table S3.Crystal data for **1o** and **1o** after 400 nm UV light irradiation for 10 second and 20 second.

	1o	1o after 400 nm UV light irradiation for 10 sec.	1o after 400 nm UV light irradiation for 20 sec.
Wavelength / Å	0.71073	0.71073	0.71073
Formula	C ₃₃ H ₃₄ F ₆ S ₂ Si ₂	C ₃₃ H ₃₄ F ₆ S ₂ Si ₂	C ₃₃ H ₃₄ F ₆ S ₂ Si ₂
formula weight	664.90	664.90	664.90
<i>T</i> / K	93 (2)	93 (2)	93 (2)
crystal system	Orthorhombic	Orthorhombic	Orthorhombic
space group	<i>Pbcn</i>	<i>Pbcn</i>	<i>Pbcn</i>
<i>a</i> / Å	18.1270 (13)	18.2115 (13) (+0.47%)	18.2662 (15) (+0.77%)
<i>b</i> / Å	10.9066 (6)	10.9601 (5) (+0.49%)	10.9946 (6) (+0.81%)
<i>c</i> / Å	33.637 (2)	33.380 (2) (-0.76%)	33.201 (3) (-1.30%)
α / °	90	90	90
β / °	90	90	90
γ / °	90	90	90
<i>V</i> / Å ³	6650.2 (8)	6662.6 (7) (+0.19%)	6667.7 (8) (+0.26%)
<i>Z</i>	8	8	8
<i>R</i> ₁ (<i>I</i> > 2 σ (<i>I</i>))	0.0465	0.0541	0.0615
<i>wR</i> ₂ (<i>I</i> > 2 σ (<i>I</i>))	0.0929	0.1122	0.1195
<i>R</i> ₁ (all data)	0.0839	0.1017	0.1276
<i>wR</i> ₂ (all data)	0.1070	0.1327	0.1462
Conversion	---	6.1%	10.0%
CCDC	1983516	1983522	1983523

Explanations of the Supplementary Movies

Supplementary movie 1

Sealability of the crystalline capsule. To ascertain that the capsule made of **1o** had a closed structure without holes, we cracked a crystal with a needle. After the capsule was broken, air bubbles entered the hollow as the liquid inside (hexane solution) began to flow out.

Supplementary movie 2

The formation process of the capsule structure. We observed the formation process of the capsule structure during the crystal growth in hexane by optical microscopy. The crystal grew from left to right. The hollows were formed parallel to the fast-growing axis similar to the recent reports of inclusions in organic molecular crystals. The formation mechanism of the crystalline capsules was in accordance with these references where the formation mechanism is attributed to the inhomogeneous growth of crystals. Due to this formation process, the solution is naturally included in the capsule. We took pictures every two minutes and combined them to make a video. The video is played at a 900x speed.

Supplementary movie 3

Release of encapsulated molecules in solution by light stimuli. When 405 nm LED light was applied to activate the capsule body of **1o**, it released encapsulated **BPEA** in hexane solution by a photosalient phenomenon. The video is played at a 16x speed.

Supplementary movie 4

Release of an encapsulated BPEA crystal by light stimuli. Upon irradiation with 405 nm LED light to the capsules, orange fluorescence from the **BPEA** crystals in the capsule was observed, followed by scattering from the crystalline capsule of **1o** to release the **BPEA** crystals by photosalient phenomena.

Supplementary movie 5

Release of encapsulated fluorescent dye in solution by light stimuli. Upon UV irradiation, the green fluorescence emission from **5(6)-FAM** was diffused in the aqueous buffer (pH = 9.18 at 25 °C) that appeared after the capsule was broken. The area of green fluorescence of **5(6)-FAM** expanded on the water surface around the crystal over time, indicating photoinduced release of **5(6)-FAM** from the crystalline capsule successfully. To simplify the observation, the crystal capsule was floated on the surface of the buffer solution. Initially, no fluorescence was observed due to the fact that the UV light was absorbed by the surface of the crystal of **1o** and did not reach inside the capsule. To eliminate the reflection of the irradiated UV light, high path filter (390 nm) was placed between the sample and the lens of a digital microscope.

Supplementary movie 6

Scattering fluorescent beads by a photosalient phenomenon. We cut off both ends of crystalline capsule with a razor blade and inserted fluorescent beads (1 μm-diameter) by a capillary effect. These crystalline capsules can scatter fluorescent beads similarly to the previous work for cup-shaped crystals by hand processing. Before irradiation of UV light, the colour of fluorescent beads was yellow. Under UV light irradiation, these beads emitted green fluorescence. The scattering speed is around 1 m/s.

Supplementary movie 7

The experiment similar to Video 5 but for a smaller capsule. The smaller capsules also released the **5(6)-FAM** they contained, which was clearly observed by the expansion of the cloud-like green fluorescent zone around the crystal upon UV irradiation.

Supplementary movie 8

Photosalient phenomenon of a crystalline capsule of **1o** by multiphoton absorption. Upon irradiation of the femtosecond NIR laser (802 nm), the crystalline capsule of **1o** was coloured blue (dark blue domain located slightly lower right from the centre is the cavity including hexane solution of **1o**). The initial crack was observed at 50 s, and the left side jumped out immediately. The second cracks were observed at 98 s. At this time, the hexane solution of **1o** in the cavity leaked out. Consequently, the area of dark blue domain is reduced. Then, the missing part of the crystal showed a photosalient phenomenon (99 s). Video speed is 16 times faster than it really is.

Supplementary movie 9

Demonstration of the dependence of the photosalient phenomena on the polarization direction of the light: case for two crystalline capsules. Two crystalline capsules of **1o** were placed orthogonally to each other on a slide glass. When 365-nm linearly polarized light was irradiated, the crystal which has its long axis perpendicular to the polarization direction showed coloration followed by jumping away. In contrast, the other crystal which has its long axis parallel to the polarization direction showed almost no change except a slight change in its colour.

Supplementary movie 10

Demonstration of the dependence of the photosalient phenomena on the polarization direction of the light: case for three crystalline capsules. Three crystalline capsules were placed together and oriented at angles 45° apart. When 365-nm linearly polarized light was irradiated, the crystal whose long axis was perpendicular to the polarization direction jumped away at first, followed by the one rotated 45° from the polarization direction. The crystal whose long axis was parallel to the polarization direction remained largely unchanged except a slight change in its colour.